Dopant effects on the photoluminescence of interstitial-related centers in ion implanted silicon

B. C. Johnson,[1,a),b)] B. J. Villis,[1] J. E. Burgess,[1] N. Stavrias,[1] J. C. McCallum,[1]
S. Charnvanichborikarn,[2] J. Wong-Leung,[2] C. Jagadish,[2] and J. S. Williams[2]
[1]*School of Physics, University of Melbourne, Victoria 3010, Australia*
[2]*Department of Electronic Materials Engineering, Research School of Physics and Engineering, The Australian National University, Canberra ACT 0200, Australia*

(Received 29 January 2012; accepted 30 March 2012; published online 10 May 2012)

The dopant dependence of photoluminescence (PL) from interstitial-related centers formed by ion implantation and a subsequent anneal in the range 175–525 °C is presented. The evolution of these centers is strongly effected by interstitial-dopant clustering even in the low temperature regime. There is a significant decrease in the W line (1018.2 meV) PL intensity with increasing B concentration. However, an enhancement is also observed in a narrow fabrication window in samples implanted with either P or Ga. The anneal temperature at which the W line intensity is optimized is sensitive to the dopant concentration and type. Furthermore, dopants which are implanted but not activated prior to low temperature thermal processing are found to have a more detrimental effect on the resulting PL. Splitting of the X line (1039.8 meV) arising from implantation damage induced strain is also observed. © *2012 American Institute of Physics*. [http://dx.doi.org/10.1063/1.4710991]

I. INTRODUCTION

Ion implantation is a central process in the fabrication of silicon devices. Interstitials and vacancies resulting from implantation evolve into a broad range of stable defects during subsequent processing. These defects have a profound effect on the electrical properties of the material. In particular, Si interstitials can cluster with dopant atoms leading to dopant transient enhanced diffusion (TED).[1,2] This remains a serious issue for the formation of shallow active profiles of boron or phosphorus. Small interstitial clusters are difficult to detect by electrical or magnetic characterization techniques but some are associated with distinct photoluminescence (PL) lines such as the W line with a zero-phonon line (ZPL) at 1018.2 meV. The W center is thought to be a tri-interstitial cluster formed by inserting three Si interstitials into the three parallel bonds surrounding a tetrahedral interstitial site.[3–6] It is present in irradiated samples independent of implanted species and its intensity thermalizes after a low temperature anneal (~250 °C). A high temperature anneal results in the aggregation of interstitial clusters to extended defects such as rod-like defects (RLDs).[7,8]

Recently, we showed that the interaction between B and self-interstitials leads to a reduction in the PL intensity of interstitial-related centers and identified a B concentration of 3.2×10^{18}cm^{-3} above which no W line is observed.[9,10] This was ascribed to either the prevention of the formation of these centers or the preferential non-radiative recombination at B-interstitial clusters (BICs). The tightly bound self-interstitials in these BICs persist to higher anneal temperatures where the formation of RLDs (and the so called R line luminescence from these defects) may also be inhibited.[11,12] The efficiency of Si electroluminescent devices based on optically active interstitial-based defects would also be compromised by this B-interaction effect.[13]

In this work, we investigate further the dopant dependence of interstitial-related PL formed by using implanted Si, P, and Ga followed by anneals up to 525 °C. Both bulk doped and dopant implanted samples are employed. Implantation of dopants allows the study of both thermally activated dopants or in their as-implanted form. Although the clustering observed here is not expected to correlate directly with TED processes in the higher temperature regime, the interactions of dopants with self-interstitials and their defect evolution are further elucidated. A standard kinetic model is shown to describe the observed enhancement of the PL under certain processing conditions and PL quenching with increased measurement temperature and the formation of alternative recombination pathways. Possible routes to realize efficient Si based light emitting diodes (LEDs) are discussed.

II. EXPERIMENTAL DETAILS

Interstitial-related defects were formed in Cz-grown (100) Si substrates with different bulk resistivities with an 80 keV Si implant to a fluence of 1×10^{14}cm^{-2} with a beam flux of 18 nA/cm^2. Samples were rotated 10° from major crystallographic planes and further tilted 7° during implantation to reduce the effect of a deeply penetrating channelling component of the incident beam. All implantations were performed on the NEC 150 kV ion implanter at the Australian National University. The implantation stage was held at room temperature for the duration of the implant. Following implantation and prior to thermal processing, the wafers were cleaned in Piranha (4:1, Sulphuric Acid and Hydrogen Peroxide) and RCA-2 (5:1:1, water, hydrogen peroxide, and hydrochloric acid) solutions. Various low temperature anneals in an Ar ambient were performed in a rapid thermal

[a)]Electronic mail: johnson.brett@jaea.go.jp.
[b)]Present address: Radiation Effects Group, Japan Atomic Energy Agency, 1233 Watanuki, Takasaki, Gunma 370-1292, Japan.

annealer (RTA) between 175 and 525 °C for 15 min to form the optically activated interstitial clusters. No specially grown surface passivation layer was used.

Dopants were also implanted into P-doped wafers with a resistivity of 5–10 Ω cm. Fig. 1(a) shows the dopant profiles as calculated with the standard analytical implantation models employed in FLOOPS-ISE™.[14] The dopant fluences and energies were adjusted so that the resulting Si recoil (interstitial) profiles are similar as shown in Fig. 1(b). A full-cascade Stopping and Range of Ions in Matter (SRIM) simulation for the B implant is shown for comparison. SRIM does not give any data points for depths beyond 250 nm as it assumes implantation into an amorphous solid. Although the sample is rotated during implantation, FLOOPS-ISE™ predicts an elongated channeling tail which is more consistent with experimental observations of off-channel implants into c-Si.[15–17] The channeling tail of the P implant is particularly prominent. The simulations do not take into account any annealing effects and recombination with vacancies so the actual interstitial concentrations are expected to be much lower than that shown in Fig. 1(b) but still greater than the bulk dopant concentration before the subsequent anneals.[18] Furthermore, the nature of the disorder will vary with the mass of the implanted ion. For B, the damage cascade will be dilute while those created by the passage of Ga through the sample will be dense.

After implantation, the samples were scribed in half. One half underwent an activation anneal in a furnace at 950 °C for 20 min in a nitrogen atmosphere. Interstitials were subsequently introduced with the 80 keV Si implant over the activated dopant profile so that the injected interstitial profile was similar to that of the dopant implanted half. Both halves then underwent the low temperature RTA anneals.

The PL measurements were performed at either 20 K in a Janis ST-500 cold finger cryostat or at 80 K in a liquid nitrogen cooled Linkam THMS600 temperature stage. The 532 nm line of a frequency doubled Nd:YAG laser was directed onto the sample with a confocal microscope equipped with a near-infrared optimized 20×, long working distance objective lens with a numerical aperture of 0.4. The focus was adjusted to achieve maximum W line intensity and collected back through the objective lens into a Renishaw InVia Reflex 0.25 m working distance micro-Raman spectrometer and a liquid nitrogen cooled InGaAs array detector. The spectral resolution is approximately 0.2 meV. Since the use of a confocal microscope resulted in high laser power densities, the measurement temperature was restricted to above 20 K in order to avoid the formation of an electron-hole droplet. In addition, the W line may decrease in intensity below 20 K depending on whether there are other defects present to compete for excitons.[19]

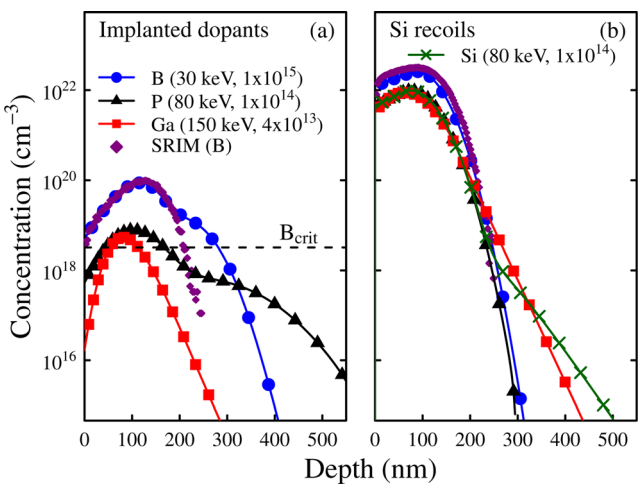

FIG. 1. (Color online) FLOOPS-ISE™ simulations of (a) the implanted dopant concentrations and (b) the resulting Si recoils created by Si, B, P, and Ga at the energies and fluences (in cm^{-2}) indicated in the figure. The interstitial concentrations of these implants are approximately equal. The critical boron concentration, B_{crit}, above which interstitial-related luminescence is not observed is indicated by the dashed line.[9] A full cascade SRIM simulation for the B implant is included for comparison (closed diamonds).

III. RESULTS

A. Bulk doped silicon

Figure 2 shows typical PL spectra of bulk doped samples after implantation with 80 keV Si to 1×10^{14} cm^{-2} followed by a RTA at 275 °C for 15 min. The band edge-related PL arising from the transverse optic free exciton (FE_{TO}) is observed around 1097 meV. However, it is the W ZPL at 1018.2 meV that dominates the spectra of all three samples. The vibronic sideband of the W line appears on the lower energy side of the ZPL. Unlike the implantation of the noble gases,[3,20] no significant difference in the ZPL peak position or width between samples with different dopants was observed. However, there is a noticeable difference in the intensities as indicated by the vibronic sideband intensity which is related to the ZPL intensity via the Huang-Rhys factor.[3] This factor is independent of substrate doping but varies with temperature. As discussed in our previous work, both implanted and bulk B has a detrimental effect on the W line intensity.[9,10] We observe the opposite behaviour for P consistent with a study by Giri.[5] The relative intensities for samples (i):(ii):(iii) is approximately 9:5:1 at this measurement and anneal temperature.

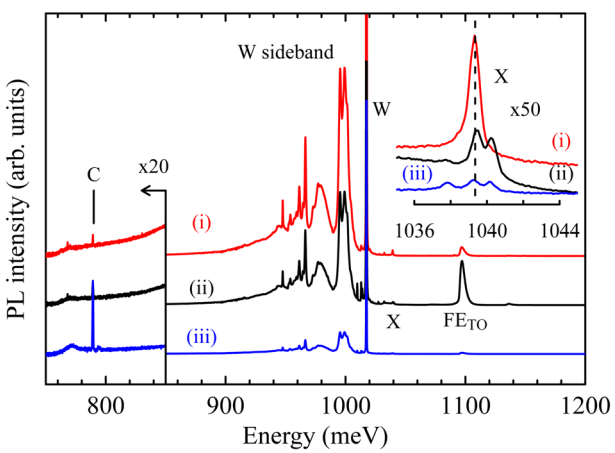

FIG. 2. (Color online) PL at 20 K from three substrates implanted with 80 keV Si to 1×10^{14} cm^{-2} and annealed at 275 °C. The background dopant and resistivity range for the three substrates are (i) P-doped 0.8–0.9 Ω cm, (ii) P-doped 5–10 Ω cm, and (iii) B-doped 5–10 Ω cm. The inset shows the X line in each spectrum multiplied by a factor of 50. The detector sensitivity rolls off at ~770 meV.

The C center is also observed at 789.4 meV and arises from a C_i-O_i cluster.[19] The C line in the B-doped substrate is about 5 times greater than that in the other two substrates suggesting either a greater carbon-oxygen content in this substrate or a smaller concentration of competing recombination centers. The C and O concentrations in Cz-grown silicon are typically $\sim 10^{16}$ cm^{-3}. In other samples in this study, the C line intensity is not observed to have an obvious dopant type or concentration dependence. The competition between C and B for O to form the C center or some B-O complex such as B_iO_{2i}[21] is not apparent. The C line intensity is also maximized at ~275 °C and tends to anneal out by 525 °C. The G line at 969.5 meV (C_s-Si_i-C_s) was not observed in the anneal temperature range considered in this work.

The inset of Fig. 2 shows a close-up view of the X line which is usually found at 1039.8 meV. The X center is a four interstitial cluster stable up to 400 °C.[6,22,23] The intensity of the X line appears to have the same dopant dependence as the W line and is observed to split into three separate peaks at 1037.8, 1039.4, and 1040.2 meV in the low P and B doped samples. Most of the intensity is contained in the central peak. The X line-shape is known to be modified by stress in a way indicative of its tetragonal symmetry.[24] In uniaxial stress measurements, the X line splits into two components when under ⟨001⟩ and ⟨011⟩ uniaxial stress while ⟨111⟩ uniaxial stress results in a redshift. Since three peaks are observed, the X centers appear to exist in two separate depth ranges having different strain fields. The central component may arise from a depth that contains little stress such as in the tail of the implant profile where the damage is more sparse. The split component is consistent with ⟨001⟩ uniaxial stress of 22 MPa. This is comparable to the global strain values found in Si implanted Si for a comparable fluence.[25] The C line is also observed here to split to various degrees under different implantation and anneal conditions. The splitting is different to the X line given the different symmetry of the defect (Monoclinic, C_{1h}[26]) and hence its response to the strain field.

In Fig. 3, the PL spectra measured at 20 and 80 K are contrasted for the B doped wafer annealed at 275, 400, and 525 °C. In these samples, the W line progressively decreases in intensity as the anneal temperature increases. By an anneal of 400 °C, it is no longer observed at 80 K although it is still prominent at 20 K. Both 400 °C spectra are instead dominated by a broad emission band centered around ~1 eV. Given the higher anneal temperature required to create this broad emission band, it is likely that it arises from larger interstitial clusters in multiple configurations.[5,22] We observe this feature to also be enhanced by P. Interestingly, this broad feature is not as susceptible to thermal quenching as the W line. Where the W ZPL decreases by over three orders of magnitude between 20 and 80 K, the broad peak decreases by only one third. After a 525 °C anneal, the W line is replaced with a series of weak broad lines between 950 and 1100 meV (on the 20 K spectrum) overlaid on a different broad emission band centered at 920 meV. Given their weak and broad nature, we have not attempted to categorize these lines. However, lines at similar energies produced under similar conditions have previously been observed by a number of authors.[5,8,27,28] Their origin is

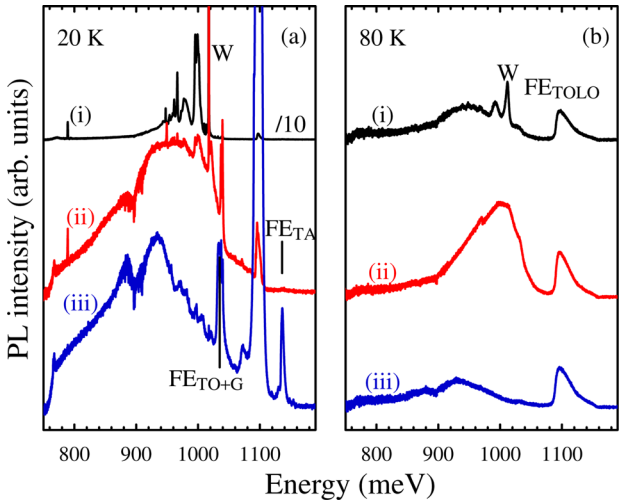

FIG. 3. (Color online) PL measured at (a) 20 K and (b) 80 K of the B-doped 5–10 Ω cm annealed at (i) 275, (ii) 400, and (iii) 525 °C for 15 min. Spectrum (a) (i) is divided by 10 for comparison. An atmospheric absorption feature is observed at around 900 meV. The band edge-related PL lines are also indicated.

not definitively known but they are usually attributed to larger interstitial clusters. Recently, it was suggested that these lines arise from the one defect (I_8) with radiative recombination between different excited states.[29] These peaks are not apparent in the 80 K spectra. The broad 920 meV band attributed to vacancies[30] is observed here to be subject to strong thermal quenching.

At 20 K, the band edge PL (FE$_{TA}$, FE$_{TO}$, and FE$_{TO+G}$) also shows different behaviour than at 80 K. Generally, the band edge PL increases with anneal temperature for all the samples studied in this work. However, at higher measurement temperatures, as carrier diffusion increases and non-radiative recombination processes start to dominate, the trend is not so obvious. The band edge-related peaks also broaden so that their various components (TO and longitudinal optic (LO) free exciton bands) merge together.

The integrated intensities at 80 K of the W ZPL and the total sub-band (750–1070 meV) PL for the bulk doped samples are plotted as a function of post-implantation anneal in Fig. 4. The optimal temperature to achieve the maximum W line intensity is 50 °C lower for the B doped samples than the highly P doped sample. We observe this trend for all samples considered in this work and will be discussed further below. The integrated sub-band PL shows a peak at 400 °C corresponding to the maximum in the broad emission band centered at 1 eV and a lower temperature shoulder corresponding to the W line. The 1 eV band has the same dopant dependence as the W-line. The most intense 920 meV peak (vacancies) was observed in the B doped sample suggesting that the formation of BICs may result in a vacancy excess.

B. Dopant implanted silicon

The spectra of a B implanted sample as a function of anneal temperature are presented in Fig. 5(b). A single B implant to a fluence of 1×10^{15}cm^{-2} is not expected to result in the W line.[10] Here, we observe the W line because

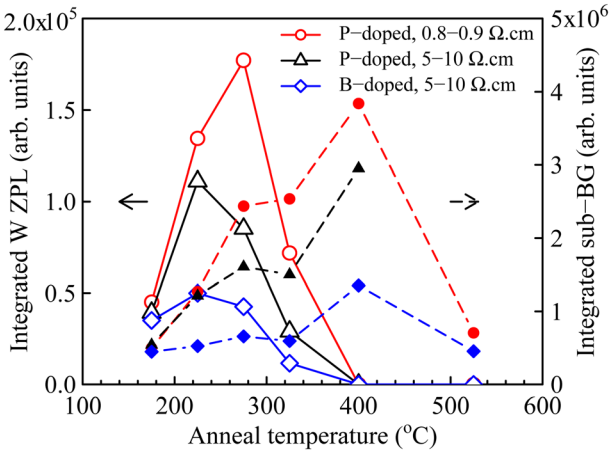

FIG. 4. (Color online) The integrated intensity of the W ZPL (open symbols plotted against the left axis) and the total sub-band edge PL (closed symbols plotted against the right axis) for the samples in Fig. 2 as a function of anneal. These data were extracted from PL measurements performed at 80 K.

of the additional interstitials injected beyond the extent of the B profile by a subsequent Si implant. Strong W, X, and Y lines can, therefore, be observed simultaneously. The W line is optimized at 225 °C as shown in Fig. 5(a). At 275 °C, the Y line appears and increases in intensity peaking at 325 °C and then quickly disappears by the 525 °C anneal consistent with previous reports.[31,32] The Y line is associated with a B_2I cluster which is similar to the W center in structure with two self-interstitials replaced by boron atoms.[33]

The X line appears after each anneal up to 400 °C. Once again, the X line is observed to split and is greatest at an anneal of 325 °C with a value of 2.3 meV (20 MPa), the temperature at which the Y line intensity is greatest.

Fine structure is observed close to the W ZPL consisting of two sets of seven lines which are fairly symmetric about the W ZPL. We attribute these to emission with the simultaneous absorption or emission of one or two phonons of different energy. The relative intensities of the lines appear to be governed by the Boltzmann factor, $\exp(\Delta E/kT)$, where ΔE is the energy shift from the W ZPL (phonon energy). The main three lines (indicated by the asterisk in Fig. 5) have $\Delta E = 4.2$, 5.3, and 8.8 meV. Additional peaks closer to the ZPL could not be resolved due to spectral broadening. The line positions, widths, and relative intensities do not appear to have any dependence on doping except for changes in the absolute intensities which scale with the W ZPL. Four fine structure lines have previously been observed at 4.2 K and attributed to the populating of W center excited states and local phonons having $\Delta E = 7$ meV.[34] It is difficult to correlate our measurements with this earlier work at this stage given the differences in experimental conditions. An additional line at 1032.4 meV is of a similar intensity to the satellite lines but its intensity does not scale with the other satellite lines. Here it is optimized at the same temperature as the W line at 225 °C. However, its intensity appears to decrease more rapidly than the W line for higher annealing temperatures suggesting that it is not part of the W line system. It may be associated with the I4 centre.[35]

The integrated W ZPL intensity in samples implanted with B, P, or Ga that have either been activated (D_{act}) or not (D_{imp}) as a function of the low temperature anneal is shown in Fig. 6. Dopant profiles and the resulting interstitial profiles for these samples were presented in Fig. 1. Those samples with an activation anneal have been further implanted with 80 keV Si to a fluence of 1×10^{14} cm^{-2} so that all samples have similar interstitial concentration profiles before the low temperature RTA.

Generally, P_{imp} and Ga_{imp} result in similar intensities to the sample without a dopant implant while P_{act} and Ga_{act} enhance the intensity. After a 225 °C anneal, the W line is enhanced by a factor of two when an activated Ga implant is present. This is the greatest W line intensity observed in this work. The B implants result in a significant reduction of the W line and other interstitial-related PL lines with the B_{imp} case having a more detrimental effect.[10] The anneal temperature at which the W-line is maximum is found to be dopant

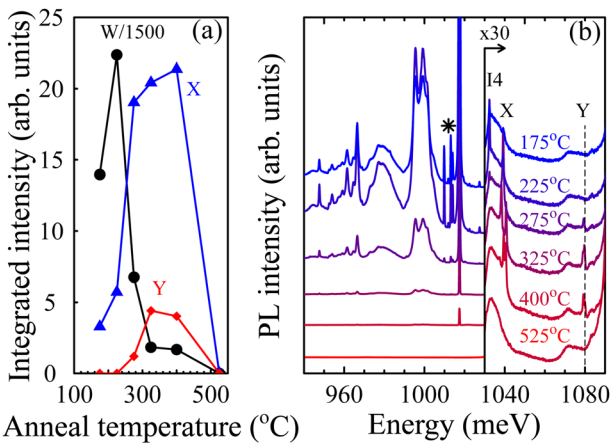

FIG. 5. (Color online) (a) Integrated intensities of the W, X, and Y lines as a function of the anneal temperature and (b) the corresponding 20 K PL spectra for a sample implanted with 30 keV B to a fluence of 1×10^{15} cm^{-2} followed by a further Si implant. The spectra have been offset vertically for clarity. The I_4, X and Y lines are indicated. Fine structure on the low energy side of the W ZPL is indicated with the asterisk.

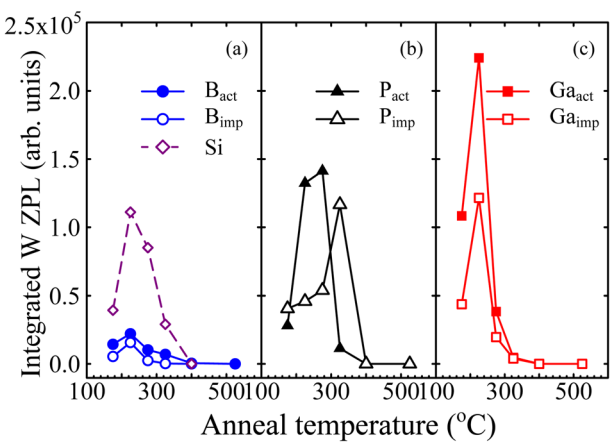

FIG. 6. (Color online) The integrated intensity of the W ZPL as a function of anneal temperature for (a) B, (b) P, and (c) Ga implanted samples with (closed symbols) and without (open symbols) an activation anneal. The implantation fluences and energies are the same as those in Fig. 1. PL measurements were performed at 80 K. A sample implanted with only Si is shown for comparison in (a).

dependent. For B and Ga, it is 225 °C. P shifts the optimum temperature up by 50–100 °C.

For the activated samples, a weak broad band centered at ~820 meV appears after a 525 °C anneal (not shown). In bulk doped samples, we find that anneal temperatures between 700 and 1000 °C are usually required to form such a band which is associated with dislocations. Interestingly, the band did not appear immediately after the activation anneal which is expected to have created extended defects. Interstitials injected with the subsequent Si implantation may have interacted with these extended defects during the low temperature anneal by an interstitial gettering mechanism.[36] Since sharp D-lines did not appear in the 20 K PL measurements, it is more likely that this band arises from the binding of interstitial clusters at extended defects.[37] At the lowest anneal temperatures studied, the interaction is expected to be small with a diffusion length of approximately 0.9 Å at 275 °C compared to 290 nm at 525 °C.[38] However, recombination is expected to take place at these extended defects given the long diffusion length of excitons in Si. Despite this, it is these very samples which produce the greatest W line intensity. We propose that the relative enhancement is due to a Fermi level effect which is elaborated upon in Sec. IV.

The W line has a strong measurement temperature dependence and is totally quenched well-below room temperature (<100 K). This limits the practical application of the W line in LED devices. For the dopant activated samples (Fig. 6), the W line intensity was also measured as a function of temperature. The intensity was found to decrease with an associated de-activation energy of (76±8) meV (Si), (48±5) meV (B), (57±3) meV (P), and (73±5) meV (Ga). The values agree well with the range of values reported in the literature.[5,13] It can be seen that when B is present, the W line quenches less readily but had the weakest intensity at all measurement temperatures.

Figure 7 compares the 20 K PL from samples with B_{act} or P_{act} activated implanted dopants after a subsequent Si implantation and an anneal at 400 °C. Both samples had dopant implantation fluences of 1×10^{15} cm^{-2}. The band edge related PL is similar for each sample at this anneal and measurement temperature. The W ZPL is nearly 3 times weaker in B_{act} than in P_{act}. The Y line is relatively bright in B_{act} so that, as the W line is quenched, the local vibrational modes of the Y line can also be seen at 975.0 (Y^{L1}) and 1049.3 meV (Y^{L2}).[33,39] The Y^{L2} mode is superimposed on the W″ mode of the W line. The two excited states of the Y line can be observed at 1082.0 and 1085.7 meV.[40] The Y-line also has a broad vibronic sideband which extends to ~950 meV. NL1 denotes lines observed in B implanted silicon arising from an as yet unknown B-related center.[41] Although the concentration of Si interstitials was initially the same, the presence of dopants has resulted in quite different X line splitting (see inset of Fig. 7) which correspond to strain values of 40 MPa and 12 MPa for the P and B implanted samples, respectively.

As noted above, extended defects resulting from the implanted dopant activation anneal can act as alternative recombination centers in competition with the W centers. The concentration of such defects is expected to increase with the implanted dopant fluence. Therefore, in additional to possible dopant effects, damage effects may also become significant. The integrated W ZPL intensity as a function of dopant implanted fluence is presented in Fig. 8. Implanted dopants have been activated and the W centers formed with a subsequent Si implant followed by a 225 °C (Fig. 8(a)) or 275 °C anneal (Fig. 8(b)). The intensities have been normalized to a Si implanted sample without a dopant implant so the damage effect remains convoluted with any dopant effects in this data set.

At 225 °C, W line intensities of the B and Ga implanted samples decrease as the fluence increases. Both Ga and P implanted samples result in an enhanced W line compared to that of the undoped sample over a narrow fluence range. A similar trend is observed at 275 °C, however, samples implanted with P first increase and then decrease with fluence with a peak at 10^{14} cm^{-2}. The rate of intensity decrease with fluence is similar for all dopants following a power law of the form $I/I_\circ \propto (N_D/10^{15}\,\text{cm}^{-2})^{\beta}$ where β is between

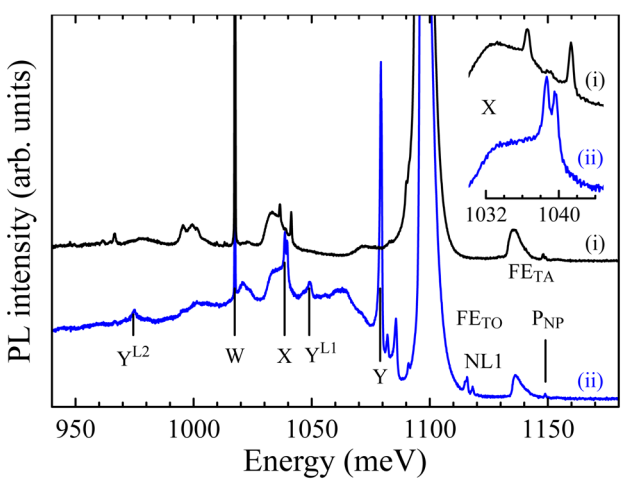

FIG. 7. (Color online) 20 K PL of samples with implanted profiles that are (i) P_{act} and (ii) B_{act} after a subsequent Si implant and a 400 °C anneal. Spectra have been offset vertically for clarity. The inset shows a close-up of the X line.

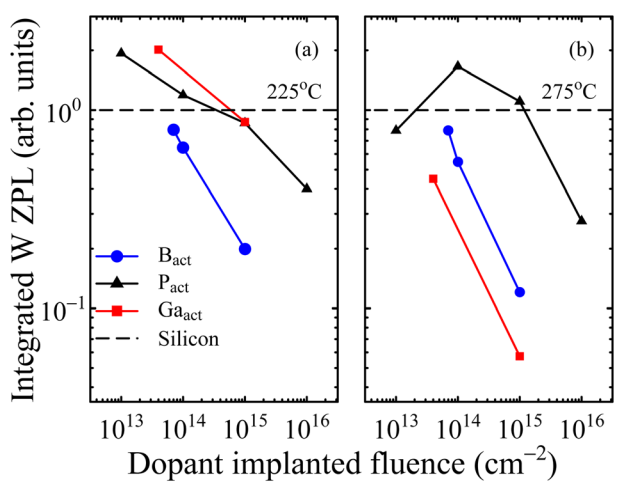

FIG. 8. (Color online) Integrated W ZPL intensity measured at 80 K as a function of the activated implanted dopant fluence normalized to the corresponding 1×10^{14}cm^{-2} Si implant intensity (dashed line) in low P bulk doped Si after (a) a 225 °C anneal and (b) a 275 °C anneal. All samples were injected with interstitials by a 1×10^{14}cm^{-2} Si implant prior to these low temperature anneals.

−0.2 and −0.7. This decrease is due to the formation of alternative non-radiative pathways such as extended defects or dopant-interstitial clusters or the inhibition of W center formation.

IV. DISCUSSION

A. Defect evolution

The W line intensity is found to be sensitive to the anneal temperature and the dopant type and concentration indicative of strong self-interstitial/dopant interactions even in the low anneal temperature regime studied here. For B, the W line intensity dependence on dopant concentration is the most significant. For all B implanted samples, the peak concentration exceeded that required to fully quench the W line (3.2×10^{18}cm^{-3}).[9,10] Therefore, the W line is not expected to emanate from depths between 0 and 300 nm. Instead, the W line arises from the channeling tail of the profile.[10] Nevertheless, under all processing conditions, the presence of B was found to be detrimental to the self-interstitial-related PL yield. This has been suggested to be a result of the prevention of W center formation or the creation of alternative non-radiative recombination pathways.[9,10] An indication for the latter is that the band edge-related PL does not correlate with the W line intensity (FE_{TO} in Fig. 2). For the B doped sample, both the FE_{TO} and the W line are weak. Exciton recombination must therefore take place non-radiatively.

The optimal anneal temperature for the W line intensity (Fig. 6) varies with dopant. For B, the sharp decrease in the W line intensity above 225 °C corresponds to an increase in the Y line (Fig. 5). As proposed by Adey *et al.*, the Y-center may form in competition with the W-center if sufficient boron is available.[33] Other BICs such as BI_2 and B_3I may also act as non-radiative recombination centers. Simulations by Aboy and Pelaz show that there is an increase in the ratio of B-interstitial clusters to Si-interstitial clusters as the anneal temperature increases.[42] Substitutional B atoms have also been found to be displaced from lattice sites during anneals in the temperature range 200–400 °C.[43] At higher temperatures (>500 °C), the B atoms return to substitutional sites. This temperature corresponds to the rapid decrease in the Y line intensity. The apparent re-activation of B atoms may compete with the formation of larger BICs in this low temperature regime. These effects cause the W line intensity versus anneal temperature curve to skew to lower temperatures.

For the heavier ions P and Ga, the denser disorder within collision cascades will lead to differences in the type and scale of disorder both following implantation and also after an activation anneal in comparison with light B ions. Thus, Si cluster formation (and hence W-line formation) will be impeded as a result of Si-interstitial trapping at this damage. The effect will increase as the implantation fluence increases, and any additional role of dopant atoms in reducing W-line intensity will be difficult to ascertain. For the heaviest dopant Ga, this may suggest that the increased residual disorder alone accounts for the large decrease in W line intensity with fluence. However, there are additional dopant effects that could be at play. For example, Ga is known to be an efficient trap for Si interstitials and has been found to quench the G line spectrum.[39] Furthermore, the activation anneal of Ga implanted to a concentration beyond its solubility limit (4×10^{19}cm^{-3})[44] is expected to give rise to strain arising from the large substitutional metastable atoms and the precipitation and clustering of Ga atoms.[45] Again the clustered dopants may result in non-radiative recombination pathways.

For the intermediate mass dopant P, there is again increasing residual disorder with increasing fluence that may ultimately reduce the W-line intensity at higher fluences in both pre-activated (and subsequent Si implanted) and non-activated P-implanted samples. In this case, a P dopant W-line enhancement effect is observed at low fluences where the damage effects are expected to be low but a damage-mediated reduction in W-line intensity may play an increasing role at higher fluences. However, other dopant atom effects could also be again at play although to a limited extent given that the anneal temperature dependence of the W line (Fig. 6) is quite different to that of B and Ga. Indeed, the interaction of P with self-interstitials is known to occur during TED.[46]

It is also found that when the W centers are formed with a single dopant implant, the W line PL intensity is less than that from samples implanted with Si over an activated implanted dopant profile (Fig. 6). This is despite the fact that implant energies and fluences were adjusted so that the injected interstitial concentration profiles were similar (Fig. 1) and the expectation that extended defects formed during the activation anneal may act as alternative recombination centers. We propose that the dominant effect here is due to a Fermi level shift. Likewise, in a narrow processing window, the implantation of P or Ga causes an enhancement of the W line intensity. This is discussed further in the following section.

B. Dopant dependence

Ion implantation results in a broad range of radiative and non-radiative traps for excitons. Consequently, the PL intensities of a particular defect are not directly related to the defect concentration. The competition between defects for excitons is also dependent on their ionization level and the sample temperature.[19] However, to understand the dopant dependence of the recombination kinetics, we make the simplifying assumption that recombination of the photogenerated excess minority carrier density, n, is dominated by recombination at the W center. In this case, the W line PL yield will be proportional to n/τ_W, where τ_W is the recombination lifetime at the W center. This can be expressed using Shockley-Read-Hall (SRH) recombination[47]

$$1/\tau_W = \frac{n_\circ + p_\circ + n}{\tau_{p\circ}(n_\circ + n_1 + n) + \tau_{n\circ}(p_\circ + p_1 + n)}, \qquad (1)$$

where $n_\circ$ and $p_\circ$ are the densities of electrons and holes in the conduction and valence bands, respectively, and are dependent on the dopant density. The SRH concentrations are $n_1 = n_c \exp((E_t - E_c)/kT)$ and $p_1 = n_v \exp((E_v - E_t)/kT)$,

where n_c and n_v are the conduction and valence band effective density of states, E_c and E_v are the conduction and valence band energies, and E_t is the energy level associated with the W center. These concentrations represent the number of electrons (holes) in the conduction (valence) band when the Fermi level is at E_t. Although the W center is fully coordinated, compressive stress is thought to give rise to a gap state close to the valence band which binds excitons.[4] Lastly, $\tau_{n\circ}$ ($\tau_{p\circ}$) is the lifetime for electrons (holes) injected into a p-type (n-type) semiconductor. In the following, it is assumed that the probability of capturing an exciton at the center is independent of temperature.

In the low injection regime, the lifetime decreases thereby increasing the PL yield as the Fermi level shifts toward either of the band edges (Fig. 9(a)). According to Eq. (1), the lifetime then becomes constant at either τ_{no} in a p-type semiconductor or τ_{po} in a n-type semiconductor. As the injected carrier densities become large, τ_W monotonically approaches $\tau_{no} + \tau_{po}$ and the dopant dependence is lost. For the samples studied above, an intermediate value is expected where a dopant dependence may still be observed.

The data from Ref. 13 for the electroluminescence intensity of the W line scaled to the zero-temperature τ_{no}/τ_W value are plotted in Fig. 9(b) and a trap energy of $E_t - E_v = 22$ meV was determined. The trends are also very similar to the model developed by Recht *et al*. to describe the thermal quenching of PL and EL and our value of $E_t - E_v$ is comparable to the electron binding energy determined in their work for the W line.[48] As the dopant density increases, it can be seen that the temperature quenching in Fig. 9(b) becomes less apparent. This may be useful in the optimization of Si-based LED devices. In addition, it is apparent from Eq. (1) that centers with E_t closer to mid-gap, such as the G, R, or D centers, are expected to act as more efficient recombination sites in agreement with Recht's model. Such centers may then be more useful in practical LED devices.

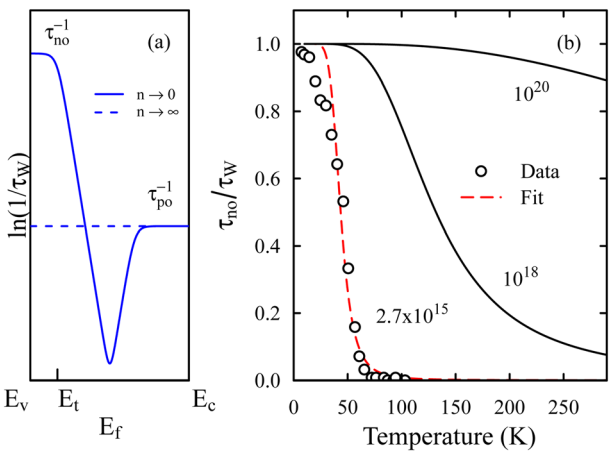

FIG. 9. (Color online) (a) The dependence of $1/\tau_W$ on the Fermi level where $\tau_{po} > \tau_{no}$ for both the low injection (solid line) and high injection (dashed line) regimes and (b) the normalized lifetime as a function of temperature for p-type Si using Eq. (1). Each curve in (b) is indicated with the majority carrier density in cm^{-3}. The data are the scaled EL W line intensity variation with temperature from Ref. 13. The fit resulted in a trap level of $E_t - E_v = 22$ meV which was used for the other curves.

In the high dopant density regime ($p_\circ \gg n_\circ$), Eq. (1) reduces to

$$1/\tau_W = \frac{1}{\tau_{no}(1 + p_1/p_o)}, \tag{2}$$

$$= \frac{A}{1 + B\exp(\Delta E/kT)}, \tag{3}$$

where $A = \tau_{no}^{-1}$, $B = n_i/N_a$, and $\Delta E = E_{fi} - E_t$ assuming that $p_o = N_a$. This equation has a similar form to the empirical formula introduced by Davies to describe the temperature dependence of the W line PL intensity.[19]

As the dopant concentration increases, Auger recombination becomes more probable with its characteristic $1/N_a^2$ dependence ($\tau_{Auger,p} \propto (N_a + 2N_a n + n^2)^{-1}$). In terms of the above dopant dependence, our data show that active P and Ga dopants do indeed enhance the W line intensity in a narrow processing window by either providing electrons to immediately combine with holes or providing holes to fill the W center gap states. However, in some cases we observe that as the dopant fluence increases the intensity starts to decrease. This occurs at a lower fluence for Ga (less than $4 \times 10^{13}/cm^{-2}$) than for P (at $1 \times 10^{14}/cm^{-2}$). As we have indicated earlier, the increase in extended defect concentration and dopant-interstitial-defect interactions with increasing fluence can account for this behaviour. Loss of W line intensity at higher dopant concentrations is furthermore expected as a result of non-radiative recombination by an Auger process. For B, the significant decrease of W line intensity with increasing fluence is attributed to the strong tendency for B atoms to cluster or to replace Si-interstitials in clusters to form non-radiative centres in preference to three-fold Si-interstitial clusters that give rise to W line luminescence.

V. SUMMARY

We have examined the formation of interstitial-related optically active centers in silicon with various bulk doped and dopant implanted samples. In all cases, B is shown to have a deleterious effect on the W line arising from competition with non-radiative recombination centers. Si-interstitials also take part in dopant clustering so that the formation of the optically active centers may be inhibited. In contrast, P increases W line luminescence and gives rise to a broad underlying band which persists to the higher anneal temperature of 400 °C. This broad band is possibly associated with larger interstitial clusters of multiple configurations. However, at P fluences greater than $1 \times 10^{14} cm^{-2}$, the PL intensity decreases as a result of increased extended defect concentration, competition of non-radiative clusters with the W line and possibly P clustering.

The optimal anneal temperature at which the W center has the greatest intensity is also lower in B and Ga implanted samples than in P implanted samples. Atomistic simulations by Aboy and Pelaz, for B, suggest that this could be due to the relative increase in the concentration of BICs at higher annealing temperatures which may act as non-radiative recombination pathways.

A basic SRH model shows that an increase in majority carrier concentration should be accompanied by an increase in the W line PL in the absence of other recombination processes. An increase was observed under a narrow processing window for P and Ga implantation. Generally, however, the PL intensity for all samples decreased with increasing implantation fluence. For P and Ga, this effect was attributed to complex interactions of damage with Si-interstitial clusters and dopant defect interactions, leading to alternate non-radiative pathways for recombination, whereas for B, dopant clustering and B atoms replacing Si-interstitials in clusters competed with the formation of three-fold interstitial clusters that give rise to W line luminescence.

ACKNOWLEDGMENTS

This work is supported by a grant from the Australian Research Council. B.C.J. is partially supported by the Japan Society for the Promotion of Science (JSPS) (Grant-in-aid for Scientific Research, 22.00802).

[1]L. Zhang, K. Jones, P. Chi, and D. Simons, Appl. Phys. Lett. **67**, 2025 (1995).
[2]P. A. Stolk, H. J. Gossmann, D. J. Eaglesham, D. C. Jacobson, C. S. Rafferty, G. H. Gilmer, M. Jaraíz, J. M. Poate, H. S. Luftman, and T. E. Haynes, J. Appl. Phys. **81**, 6031 (1997).
[3]G. Davies, E. C. Lightowlers, and Z. Ciechanowskat, J. Phys. C **20**, 191 (1987).
[4]B. Coomer, J. Goss, R. Jones, S. Öberg, and P. Briddon, Physica B **273–274**, 505 (1999).
[5]P. K. Giri, Semicond. Sci. Technol. **20**, 638 (2005).
[6]J. P. Leitão, A. Carvalho, J. Coutinho, R. N. Pereira, N. M. Santos, A. O. Ankiewicz, N. A. Sobolev, M. Barroso, J. L. Hansen, A. N. Larsen, and P. R. Briddon, Phys. Rev. B **84**, 165211 (2011).
[7]S. Coffa, S. Libertino, and C. Spinella, Appl. Phys. Lett. **76**, 321 (2000).
[8]D. C.Schmidt, B. G. Svensson, M. Seibt, C. Jagadish, and G. Davies, J. Appl. Phys. **88**, 2309 (2000).
[9]S. Charnvanichborikarn, B. J. Villis, B. C. Johnson, J. Wong-Leung, J. C. McCallum, J. S. Williams, and C. Jagadish, Appl. Phys. Lett. **96**, 051906 (2010).
[10]J. C. McCallum, B. J. Villis, B. C. Johnson, N. Stavrias, J. E. Burgess, S. Charnvanichborikarn, J. Wong-Leung, J. S. Williams, and C. Jagadish, Phys. Status Solidi A **208**, 620 (2010).
[11]T. E. Haynes, D. J. Eaglesham, P. A. Stolk, H.-J. Gossmann, D. C. Jacobson, and J. M. Poate, Appl. Phys. Lett. **69**, 1376 (1996).
[12]S. Solmi, L. Mancini, S. Milita, M. Servidori, G. Mannino, and M. Bersani, Appl. Phys. Lett. **79**, 1103 (2001).
[13]J. Bao, M. Tabbal, T. Kim, S. Charnvanichborikarn, J. S. Williams, M. J. Aziz, and F. Capasso, Opt. express **15**, 6727 (2007).
[14]FLOOPS-ISE, ISE TCAD, Release 9.5, (ISE Integrated Systems Engineering AG, Zurich, 2004).
[15]S. Yang, S. Morris, S. Tian, K. Parab, and A. Tasch, Jr., IEEE Trans. Semicond. Manuf. **9**, 49 (2002).
[16]M. Posselt, Nucl. Instrum. Methods Phys. Res. B **96**, 163 (1995).
[17]S. Tian, J. Appl. Phys. **93**, 5893 (2003).
[18]A. P. Knights, F. Malik, and P. G. Coleman, Appl. Phys. Lett. **75**, 466 (1999).
[19]G. Davies, Phys. Rep. **176**, 83 (1989).
[20]N. Bürger, K. Thonke, R. Sauer, and G. Pensl, Phys. Lett. **52**, 1645 (1984).
[21]J. Schmidt and K. Bothe, Phys. Rev. B **69**, 024107 (2004).
[22]B. Coomer, J. Goss, R. Jones, S. Öberg, and P. Briddon, J. Phys. Condens. Matter **13**, L1 (2001).
[23]R. Harding, G. Davies, P. Coleman, C. Burrows, and J. Wong-Leung, Physica B **340–342**, 738 (2003).
[24]Z. Ciechanowska, G. Davies, and E. C. Lightowlers, Solid State Commun. **49**, 427 (1984).
[25]Y. Zhong, C. Bailat, R. S. Averback, S. K. Ghose, and I. K. Robinson, J. Appl. Phys. **96**, 1328 (2004).
[26]C. P. Foy, Physica B **116**, 276 (1983).
[27]S. Libertino, S. Coffa, and J. L. Benton, Phys. Rev. B **63**, 195206 (2001).
[28]M. Nakamura and S. Murakami, J. Appl. Phys. **94**, 3075 (2003).
[29]Y. Yang, R.-D. Yang, L. Li, and F. Xiong, Chin. Phys. B **20**, 026802 (2011).
[30]G. Davies, S. Hayama, L. Murin, R. Krause-Rehberg, V. Bondarenko, A. Sengupta, C. Davia, and A. Karpenko, Phys. Rev. B **73**, 165202 (2006).
[31]R. Sauer and J. Weber, Physica B **116**, 195 (1982).
[32]K. Terashima and M. Horikawa, Physica B **376–377**, 137 (2006).
[33]J. Adey, J. P. Goss, and R. Jones, Phys. Rev. B **67**, 245325 (2003).
[34]V. Tkachev and A. Mudryi, J. Appl. Spectrosc. **29**, 1485 (1978).
[35]C. G. Kirkpatrick, J. R. Noonan, and B. G. Streetman, Radiat. Eff. Defects Solids **30**, 97 (1976).
[36]R. D. Goldberg, J. S. Williams, and R. G. Elliman, Phys. Rev. Lett. **82**, 771 (1999).
[37]A. Blumenau, R. Jones, S. Öberg, P. Briddon, and T. Frauenheim, Phys. Rev. Lett. **87**, 1 (2001).
[38]G. B. Bronner and J. D. Plummer, J. Appl. Phys. **61**, 5286 (1987).
[39]K. Thonke, N. Burger, G. Watkins, and R. Sauer, in Proc. 13th Int. Conf. Defects in Semiconductors (Metallurgical Society of AIME, New York, 1984), p. 823.
[40]K. Thonke, J. Weber, J. Wagner, and R. Sauer, Physica B + C, **116**, 252 (1983).
[41]J. Kooten, T. Gregorkiewicz, A. Blaakmeer, and C. Ammerlaan, J. Phys. C: Solid State Phys., **20**, 2183 (1987).
[42]M. Aboy, I. Santos, L. Pelaz, L. Marques, and P. Lopez, in *2011 Spanish Conference on Electron Devices (CDE)* (IEEE, 2011), pp. 1–4.
[43]G. Fladda, K. Bjorkqvist, L. Eriksson, and D. Sigurd, Appl. Phys. Lett. **16**, 313 (1970).
[44]F. A. Trumbore, Bell Syst. Tech. J. **39**, 205 (1960). Available at: http://www.alcatel-lucent.com/bstj/vol39-1960/articles/bstj39-1-205.pdf.
[45]B. M. Arora, J. M. Castillo, M. B. Kurup, and R. P. Sharma, J. Electron. Mater. **1**, 845 (1981).
[46]N. E. B. Cowern, D. J. Godfrey, and D. E. Sykes, Appl. Phys. Lett. **49**, 1711 (1986).
[47]W. Shockley and W. T. Read, Phys. Rev. **87**, 835 (1952).
[48]D. Recht, F. Capasso, M. J. Aziz, Appl. Phys. Lett. **94**, 251113 (2009).